EARTHQUAKE ENGINEERING AND STRUCTURAL DYNAMICS, VOL. 26, 61–77 (1997)

DYNAMIC RESPONSE OF EQUIPMENT IN STRUCTURES WITH SLIDING SUPPORT

L. Y. LU

National Center for Research on Earthquake Engineering (NCREE), No. 1, Sec. 4, Roosevelt Rd., Taipei, Taiwan, R. O. C.

AND

Y. B. YANG

Department of Civil Engineering, National Taiwan University, Taipei, Taiwan, R. O. C.

SUMMARY

The dynamic behaviour of a single degree-of-freedom (DOF) equipment mounted on a sliding primary structures subjected to harmonic and earthquake ground motions is studied numerically. To deal with the discontinuity nature of sliding structural systems, in this work the fictitious spring model is adopted. With the problem formulated in a state space form, an incremental numerical scheme capable of dealing with multi-DOF sliding structural systems is proposed for solving the time history responses. Numerical examples excited by harmonic and real earthquake ground motions are considered in order to study the following three effects: (1) the variation of the frictional coefficient of the sliding support, (2) subharmonic resonance and (3) effect of tuning (i.e. when the frequency of the equipment is coincident with or close to the fundamental frequency of the primary structure) on the mounted equipment. The dynamic characteristics of the mounted equipment are highlighted in the analysis of the numerical examples.

KEY WORDS: sliding support; equipment response; nonlinear system

INTRODUCTION

Sliding structures are one kind of base-isolated structure systems. By implementing a sliding support under the base raft of the structure, the transmission of seismic excitation to the structure can be greatly reduced. Westermo and Udwadia[1] are among the first researchers to study a sliding system with an oscillating single DOF superstructure placed on a sliding foundation. Based on their analytical solution for the oscillator subjected to a harmonic ground motion, they have pointed out that the sliding system will possess a very special feature, called the subharmonic resonance, as can be identified by the fact that there are several resonant peaks, in addition to the main peak associated with the main resonant frequency in the frequency response curve. Mostaghel *et al.*[2] and Mostaghel and Tanbakuchi[3] also studied a similar sliding system, using a semi-analytical solution procedure to compute the response for harmonic and earthquake ground motions. Qamaruddin[4] proved experimentally the effectiveness of sliding supports in the protection of masonry buildings from seismic attacks. Hernried and Lei[5] studied the response of an equipment mounted on a primary structure isolated by a resilient friction base. In order to study multi-DOF sliding structure systems, Yang *et al.*[6] and Lu and Yang[7] adopted a fictitious spring to represent the frictional effect of the sliding device. Their results indicated that the sliding device is effective in reducing the seismic response of MDOF structures as well.

The motion of a sliding structure may be characterized by two different phases, namely, the sliding and non-sliding phases. Although in each phase the sliding structure can be modelled as a linear system, the governing equations for the two phases are different. It is obvious that the overall behaviour of the sliding structure is non-linear. Due to the non-linearity, the subharmonic resonance is present in the frequency

CCC 0098–8847/97/010061–17

Received 16 January 1996
Revised 16 July 1996

response of sliding structures, thereby making their dynamic responses much complicated. While the effectiveness of sliding devices in seismic isolation has been studied by a number of researchers, this work aims to investigate the dynamic behaviour of an equipment item mounted on a sliding primary structure.

MATHEMATICAL MODEL AND FORMULATION

A sliding primary structure with an attached equipment can be considered as a combined structural system. In this work, the primary structure is assumed to be an n-storey shear-type building structure and an equipment as a single-DOF system which is attached to one of the floor slabs. Such a system may be schematically represented as in Figure 1. Other assumptions made in this study include (1) the frictional mechanism is of the Coulomb type, i.e. the maximum frictional force is equal to the multiplication of the frictional coefficient and the total weight above the sliding surfaces; (2) the frictional coefficient between the sliding surfaces remains constant throughout the motion of the structure, namely, the dynamic frictional force is set equal to the maximum static frictional force and (3) only horizontal ground motions are considered.

As mentioned earlier, a sliding structure may exhibit the sliding and non-sliding phases. In the non-sliding phase, there is no relative motion between the base raft and ground. This implies that the motion of the base raft is identical to the ground motion. Therefore, the DOF associated with the base raft may be removed, and the structural system has a total of $n + 1$ DOFs, with n DOFs for the primary structure and 1 DOF for the equipment. On the other hand, the total number of DOFs needed to describe the response of the structural system in sliding phase is $n + 2$, with one more DOF added for the base raft. In a finite-element-based numerical analysis, this disagreement on the number of DOFs due to the transition from one phase to the other may cause certain inconveniences. To overcome this problem, the fictitious spring model proposed by Yang *et al.*[6] for modelling the sliding structure will be adopted.

As shown in Figure 2, a fictitious spring is introduced between the base raft and the ground to represent the friction effect. As suggested by Yang *et al.*,[6] the spring constant k_f is taken as zero for the sliding phase and as a very large number for the non-sliding phase. With this model, the DOF associated with the base raft is preserved throughout the entire analysis process. In the non-sliding phase, the internal force of the fictitious spring will automatically account for the actual static frictional force which is required to balance the inertial force exerted by the superstructure.

When the structure depicted in Figure 2 is subjected to a ground motion, its dynamic equation can be expressed as

$$\mathbf{M}\ddot{\boldsymbol{\xi}} + \mathbf{C}\dot{\boldsymbol{\xi}} + \mathbf{K}\boldsymbol{\xi} = -\mathbf{M}\mathbf{l}\ddot{x}_0 + \mathbf{f} \tag{1}$$

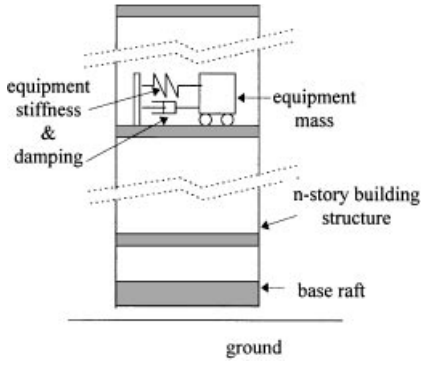

Figure 1. Combined equipment and sliding structural system

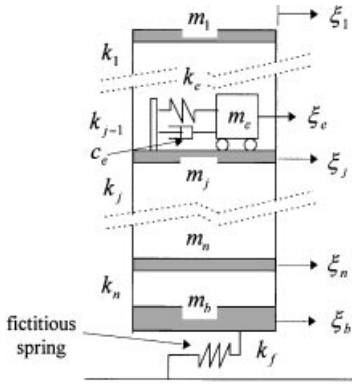

Figure 2. Sliding structure with fictitious spring model

where the $(n + 2) \times 1$ column matrix $\boldsymbol{\xi} = \{\xi_1, \xi_2, \ldots, \xi_n, \xi_b, \xi_e\}^T$ contains the relative displacements of the storey slabs as well as the relative displacement of the equipment to the ground, and the $(n + 2) \times (n + 2)$ matrices **M**, **C**, and **K** represent, respectively, the mass, damping and stiffness matrices of the combined structural system. In particular, the **M** and **K** matrices may be shown as

$$\mathbf{M} = \begin{bmatrix} m_1 & & \cdots & 0 & 0 \\ & m_2 & & \vdots & \vdots \\ & & \ddots & \vdots & \vdots \\ & \text{Symm.} & & m_b & \\ & & & & m_e \end{bmatrix} \tag{2}$$

and

$$\mathbf{K} = \begin{bmatrix} k_1 & -k_1 & 0 & \cdots & 0 & \cdots & 0 \\ & (k_1 + k_2) & -k_2 & & \vdots & & 0 \\ & & \ddots & & & & \vdots \\ & & & (k_{j-1} + k_j + k_e) & -k_j & \cdots & -k_e \\ & & & & \ddots & & \\ & \text{Symm.} & & & & (k_n + k_f) & 0 \\ & & & & & & k_e \end{bmatrix} \tag{3}$$

Note that in equation (3), the spring constant k_f for the fictitious spring and the stiffness k_e for the mounted equipment are introduced in the combined stiffness matrix **K**. The first term $\mathbf{Ml}\ddot{x}_0$ on the right-hand side of equation (1) represents the inertial force acting on each DOF due to the ground acceleration $\ddot{x}_0$, and the second term **f** is used to account for the dynamic frictional force. The column matrices **l** and **f** may be expressed as

$$\mathbf{I} = \begin{Bmatrix} 1 \\ 1 \\ \vdots \\ 1 \end{Bmatrix}_{1 \times (n+2)} \tag{4}$$

and

$$\mathbf{f} = \begin{Bmatrix} 0 \\ \vdots \\ 0 \\ -\operatorname{sgn}(\dot{\xi}_b) F_d \end{Bmatrix} \tag{5}$$

where the symbol $\operatorname{sgn}(\cdot)$ means taking the same sign of $(\cdot)$, and F_d denotes the dynamic frictional force under the base raft. Based on the assumption made in the previous section, F_d is assumed equal to the maximum static frictional force denoted by F_{max}. The term $\mathbf{f}$ must be added in equation (1), since in the sliding phase the spring constant k_f is taken as zero, in which case the fictitious spring provides no spring force to account for the constant dynamic frictional force.

From above discussion, one shall note that equation (1) can be used to describe the response of the sliding structure, either in the non-sliding or sliding phase. However, equation (1) must be subjected to two constraints, i.e.

$$\mathbf{f} = 0 \quad \text{for non-sliding phase} \tag{6a}$$

$$\mathbf{K}(k_f) = \mathbf{K}(0) \quad \text{for sliding phase} \tag{6b}$$

Note that in equation (6b), the stiffness matrix $\mathbf{K}$ is written as a function of k_f to signify the fact that all the elements except k_f in the $\mathbf{K}$ matrix remain unchanged throughout the entire motion of the structure.

Equation (1) can be further rewritten in a state space form,

$$\dot{\mathbf{x}} = \mathbf{A}\mathbf{x} + \mathbf{u} + \mathbf{p} \tag{7}$$

where $\mathbf{x}$ contains the relative displacement vector and the relative velocity vector, i.e.

$$\mathbf{x} = \begin{Bmatrix} \dot{\boldsymbol{\xi}} \\ \boldsymbol{\xi} \end{Bmatrix} \tag{8}$$

and $\mathbf{A}$ is a $2(n+2) \times 2(n+2)$ system matrix

$$\mathbf{A} = \begin{bmatrix} -\mathbf{M}^{-1}\mathbf{C} & -\mathbf{M}^{-1}\mathbf{K} \\ \mathbf{I} & \mathbf{0} \end{bmatrix} \tag{9}$$

The two force terms in equation (7), namely, $\mathbf{u}$ and $\mathbf{p}$, can be explicitly written as

$$\mathbf{u} = \begin{Bmatrix} -\mathbf{l}\ddot{x}_0 \\ \mathbf{0} \end{Bmatrix} \tag{10}$$

$$\mathbf{p} = \begin{Bmatrix} \mathbf{M}^{-1}\mathbf{f} \\ \mathbf{0} \end{Bmatrix} \tag{11}$$

Accordingly, the two conditions listed in equation (6) can be replaced by

$$\mathbf{p} = \mathbf{0} \quad \text{for non-sliding phase} \tag{12a}$$

$$\mathbf{A}(k_f) = \mathbf{A}(0) \quad \text{for sliding phase} \tag{12b}$$

Note that in equation (12b), the system matrix $\mathbf{A}$ is written as a function of k_f to signify the fact that all the elements except k_f in $\mathbf{A}$ remain unchanged throughout the entire motion of the structure.

INCREMENTAL ANALYSIS PROCEDURE

Based on the above formulas derived, the numerical scheme used in later numerical simulation is discussed in this section.

Discritized general solution

Equation (7) is similar in form to that of the linear time-invariant system. However, with the constraints (12a) and (12b) imposed, it actually represents two sets of equations for the two different phases of motion. Equations (7) and (12a) describe the motion of the structure in the non-sliding phase, while equations (7) and (12b) are valid for the structure in the sliding phase. As a sliding system may switch between these two phases at certain instants (to be discussed later), the entire behaviour of the system should undoubtedly be regarded as non-linear. Nevertheless, within each phase of motion, the system represented either by equations (7) and (12a) or equations (7) and (12b) is a linear one. It follows that the time response solution for any given phase can be denoted by

$$\mathbf{x}(t) = \mathrm{e}^{\mathbf{A}(t-t_\mathrm{i})}\mathbf{x}(t_\mathrm{i}) + \int_{t_i}^{t} \mathrm{e}^{\mathbf{A}(t-\tau)}[\mathbf{u}(\tau) + \mathbf{p}]\,\mathrm{d}\tau, \quad t_\mathrm{i} < t \leqslant t_\mathrm{f} \tag{13}$$

where $\mathrm{e}^{\mathbf{A}t}$, called the transition matrix, is a matrix exponential function of $\mathbf{A}$ and t. Also, in equation (13), t_i, t_f and $\mathbf{x}(t_\mathrm{i})$ denote, respectively, the starting time, ending time and initial conditions for the given phase. Note that the force vector $\mathbf{p}$ is not a function of time. Once the sliding system completes this phase, it will switch to the other phase. During such a transition, the final conditions $\mathbf{x}(t_\mathrm{f})$ of the current phase should be regarded as the initial conditions $\mathbf{x}(t_\mathrm{i})$ of the next phase.

Before it can be used in numerical analysis, equation (13) has to be discretized. Let the time step be denoted Δt, which is taken as a very small constant. Assuming that the inertial force vector $\mathbf{u}(t)$ is constant within each time step Δt, we can have the solution $\mathbf{x}(t)$ expressed in the following incremental form:[8]

$$\mathbf{x}_{k+1} = \mathrm{e}^{\mathbf{A}\Delta t}\mathbf{x}_k + \left(\int_0^{\Delta t} \mathrm{e}^{\mathbf{A}\tau}\,\mathrm{d}\tau\right)(\mathbf{u}_k + \mathbf{p}) \tag{14}$$

where $\mathbf{x}_k$ and $\mathbf{u}_k$ denote the values of $\mathbf{x}(t)$ and $\mathbf{u}(t)$ at the kth time step. Equation (14) states that the solution for the current step $\mathbf{x}_{k+1}$ can be computed from the solution of the previous step $\mathbf{x}_k$, plus the force terms $(\mathbf{u}_k + \mathbf{p})$. Note that once the time step size Δt is chosen, the transition matrix $e^{\mathbf{A}\Delta t}$ and its integral $\int_0^{\Delta t} \mathrm{e}^{\mathbf{A}\tau}\,\mathrm{d}\tau$ can be computed, both of which remain constant for each phase, as such, they need only be computed once during each phase.

Conditions for transition from non-sliding phase to sliding phase

The condition for a sliding system to remain in the non-sliding phase is that the static resisting force under the base raft, denoted by F_s, must be less than the maximum friction force F_max, which is equal to the product of the static frictional coefficient and the total weight of the system. Once the static frictional force reaches this maximum value, the system starts to slide. With the fictitious spring model, the static frictional force is computed as the spring force of the fictitious spring. Therefore, the condition for the sliding system to transfer from the non-sliding phase to the sliding phase can be expressed as

$$F_\mathrm{s} = k_\mathrm{f} \cdot \varepsilon(t_0) = F_\mathrm{max} \tag{15}$$

where t_0 denotes the time when the structure starts to slide, and $\varepsilon(t)$ the elongation of the fictitious spring, which is related to the relative displacement of base raft ξ_b. By using a relatively large value for the fictitious spring constant, the spring elongation will remain negligibly small during the non-sliding phase.

The exact value of transition time t_0 cannot be immediately determined using the incremental process described above. It is likely that the spring force is less than F_max at the current time step, say t_k, while exceeding F_max at the next time step t_{k+1}. In this case, since the transition time t_0 is confined within the time interval (t_k, t_{k+1}), one may employ numerical methods, such as the bisection method or Newton's method to solve equation (15) for the exact transition time t_0 to a desired accuracy.

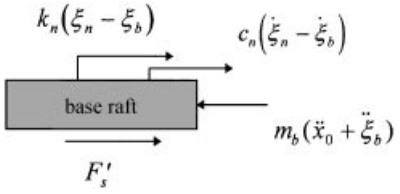

Figure 3. Free body diagram of base raft

Conditions for transition from sliding phase to non-sliding phase

After the structure enters the sliding phase, it may return to the non-sliding phase whenever the following two conditions are satisfied: (1) the relative velocity of the base raft to the ground reaches zero, i.e. $\dot{\xi}_b = 0$ and (2) the equivalent static frictional force, denoted by F_s', is less than the maximum static frictional force F_{max}. Considering the free body diagram of the base raft shown in Figure 3, the equivalent static frictional force F_s' can be computed by

$$F_s' = m_b \ddot{x}_0 - k_n(\xi_n - \xi_b) - c_n \dot{\xi}_n \tag{16}$$

This is exactly the force required to balance the motion of the superstructure in the non-sliding phase, based on the fact that the base raft and the ground have the same acceleration and velocity (i.e. $\ddot{\xi}_b = \dot{\xi}_b = 0$). For the system to transfer from the sliding phase to non-sliding phase, both conditions must be satisfied simultaneously. It may happen that only the first condition is satisfied, while the computed F_s' is larger than F_{max}. For this case, the sliding system will not enter the non-sliding phase, but reverse its direction of sliding. Correspondingly, the actual frictional force F_s should be set equal to the dynamic frictional force, rather than the equivalent static force F_s'. On the other hand, if both conditions are satisfied, the system will enter the non-sliding phase. It follows that F_s should be set equal to F_s' and used as the initial frictional force. With this initial condition, the initial elongation $\varepsilon(t_i)$ of the fictitious spring and the initial relative displacement $\xi_b(t_i)$ of the base raft can be computed, and applied to the non-sliding phase that follows.

NUMERICAL RESULTS AND DISCUSSION

The aforementioned numerical method has been applied to investigating the response of the equipment mounted on sliding structures excited by both harmonic and earthquake ground motions. In the two numerical examples that follow, a single-DOF equipment is mounted on the roof of a sliding building structure. The sliding primary structure is considered to be a single storey building only, in order to focus on the response of equipment. However, it should be clear that the proposed numerical method is suitable for dealing with any multi-DOF sliding structural system. The following discussion will be concentrated on three aspects, namely, the effect of frictional coefficients, subharmonic resonance and the tuning effect.

Harmonic excitation

Some parameters for the structural properties of the single DOF building are: mass of base raft $m_b = 2{\cdot}72$ kg $(=6$ lb); mass of structure $m_s = 0{\cdot}91$ kg $(=2$ lb); structural stiffness $k_s = 13827{\cdot}95$ N/m $(=78{\cdot}96$ lbf/in); mass ratio of equipment to structure $m_e/m_s = 1/100$; fictitious spring constant $k_f = 10\,000k_s$; structural damping $c_s = 220{\cdot}66$ N sec/m $(=1{\cdot}26$ lbf sec/in, equal to a damping ratio $\zeta_s = 5$ per cent); equipment damping ratio $\zeta_e = 5$ per cent. Using the above chosen parameters, the primary structure has an undamped natural frequency $f_s = 1{\cdot}0$ Hz in the non-sliding phase, and of $f_s^* = 1{\cdot}15$ Hz in the sliding phase (hereafter, a star sign $*$ on an entity indicates that the entity is associated with the sliding phase). For the case of harmonic excitation, a harmonic ground acceleration of $\ddot{x} = 0{\cdot}5g \sin 2\pi f_g t$ with a driving frequency of f_g will be considered throughout this study. By varying the frequency f_g, the frequency response for the acceleration of the mounted equipment can be studied.

Effect of frictional coefficient. In order to study the effect of frictional coefficients, the frequency responses of the acceleration of the equipment have been plotted in Figures 4 and 5 for four different frictional coefficients, $\mu = 0{\cdot}4$, $0{\cdot}25$, $0{\cdot}1$ and $0{\cdot}05$. The only difference between Figures 4 and 5 is the chosen equipment natural frequency f_e, which is taken as $0{\cdot}5$ and 5 Hz for Figures 4 and 5, respectively, to represent relatively soft and stiff equipments. Four observations can be made from these figures: (1) The use of a smaller frictional coefficient generally will reduce the acceleration response of the equipment in comparison with the fixed base case. (2) Besides the main resonant response around 1 Hz, there are extra peaks appearing in the range of lower excitation frequencies. These are nothing but the response of subharmonic resonance. With a large frictional coefficient, say, with $\mu = 0{\cdot}25$ or $0{\cdot}4$, the subharmonic resonant response may exceed the response of a fixed base case. (3) The main resonant frequency associated with the natural frequency of the primary structure drifts from f_s toward f_s^*, as the frictional coefficient μ changes from ∞ (for fixed base case) to $0{\cdot}05$, while the subharmonic resonant frequencies remain basically unchanged. (4) As can be seen from Figure 5, in the range of lower ground frequencies, i.e. $0{\cdot}1 \sim 0{\cdot}35$ Hz, the response for a stiff equipment with a frictional coefficient of $\mu = 0{\cdot}25$ is higher than that of $\mu = 0{\cdot}4$, implying the response for a sliding system with a larger frictional coefficient is closer to that of a fixed base case.

Subharmonic resonance. From Figures 4 and 5, one may also note that subharmonic resonance only occurs at frequencies lower than the equipment's natural frequency. A similar observation was also made by Westermo and Udwadia[1] in their analytical study for a single-DOF sliding oscillator. They concluded that the subharmonic resonance will only occur at excitation frequencies lower than that of the oscillator. Using the same soft and stiff equipments mentioned earlier, such a phenomenon can be more clearly observed in

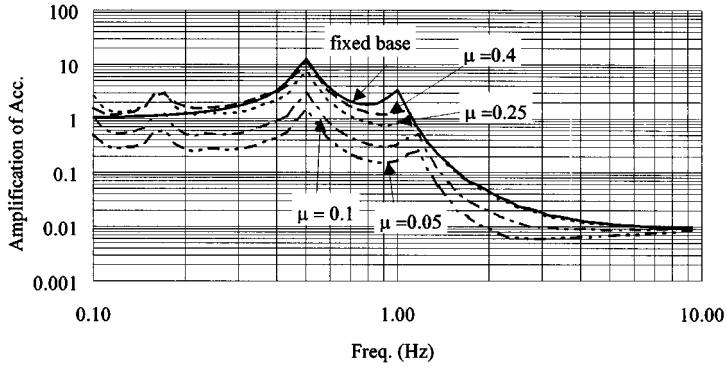

Figure 4. Frequency responses of equipment with various μ values ($f_e = 0{\cdot}5$ Hz; $f_s = 1$ Hz; $f_s^* = 1{\cdot}15$ Hz)

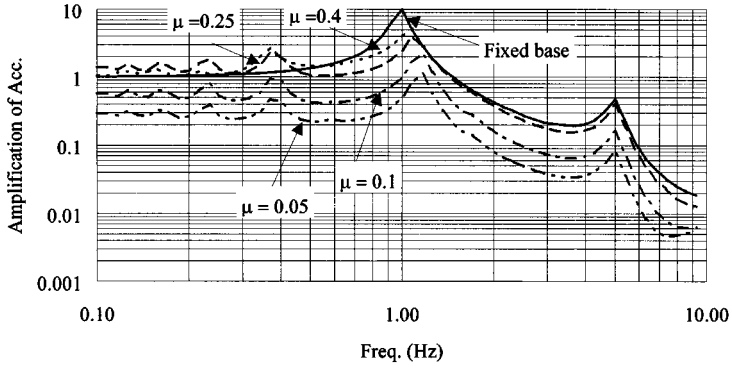

Figure 5. Frequency responses of equipment with various μ values ($f_e = 5$ Hz; $f_s = 1$ Hz; $f_s^* = 1{\cdot}15$ Hz)

Figures 6 and 7, in which both the structure and equipment responses are depicted for the case of $\mu = 0{\cdot}1$. For the case where the equipment frequency (0·5 Hz) is lower than that of the structure (1 Hz), the equipment exhibits a subharmonic behaviour very different from that of the primary structure (Figure 6). On the other hand, for the case where the equipment has a frequency (5 Hz) higher than that of the structure, the difference between the responses of the equipment and the structure is considerably smaller (Figure 7). The reason for this is that for lower excitation frequencies the equipment behaves like a rigid system and moves with the structure, while for higher excitation frequencies the primary structure serves as a soft isolator to the equipment.

Effect of tuning. By tuning, one means that the frequencies of the equipment and structure are identical or very close. In order to study this effect, the frequency of the equipment is chosen to be $f_e = 1{\cdot}1$ Hz so that it falls between the natural frequencies of the non-sliding phase and sliding phase, i.e. f_s and f_s^*. Comparing Figure 8 for the tuning case with Figure 5 for the non-tuning case, one may conclude that when f_e is tuned to f_s (or f_s^*), the response of the equipment is drastically amplified for as large as three times both at the main resonance frequency (around f_e) and at the subharmonic resonance frequencies.

Figure 9 illustrates how the equipment response varies with f_e, when the ground frequency f_g is fixed at 0·5 Hz. The following observations can be made from the figure: (1) When f_e is adjusted to f_g, the response reaches its maximum for any given value of μ. (2) The effect of sub-harmonic resonance causes the response to be amplified when f_e is tuned to about 1·3 Hz, implying a ratio of f_g/f_e around 0.38 (similar to the ratio f_g/f_e for the first subharmonic frequency in Figure 8).

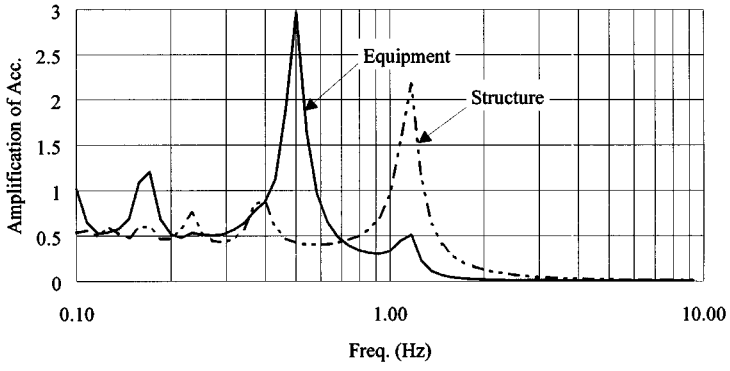

Figure 6. Structure and equipment frequency responses ($\mu = 0{\cdot}1$; $f_e = 0{\cdot}5$ Hz; $f_s = 1$ Hz; $f_s^* = 1{\cdot}15$ Hz)

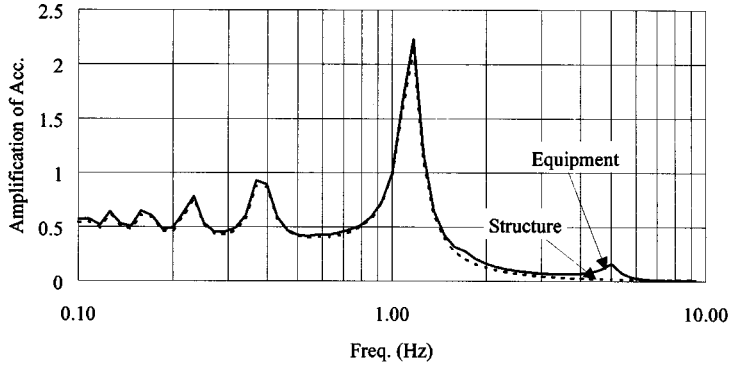

Figure 7. Structure and equipment frequency responses ($\mu = 0{\cdot}1$; $f_e = 5$ Hz; $f_s = 1$ Hz; $f_s^* = 1{\cdot}15$ Hz)

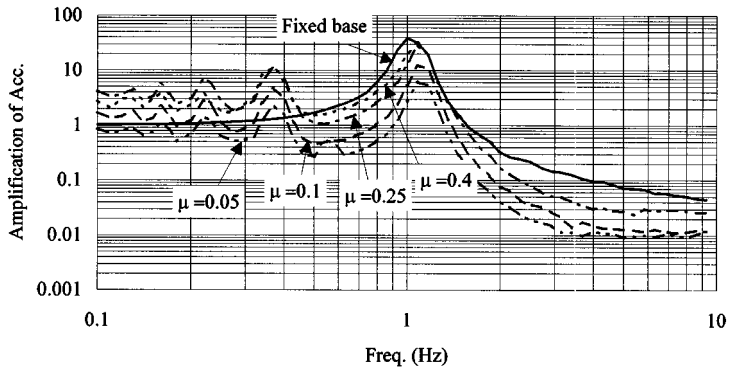

Figure 8. Frequency responses of equipment tuned to the structure frequency ($f_e = 1{\cdot}1$ Hz; $f_s = 1$ Hz; $f_s^* = 1{\cdot}15$ Hz)

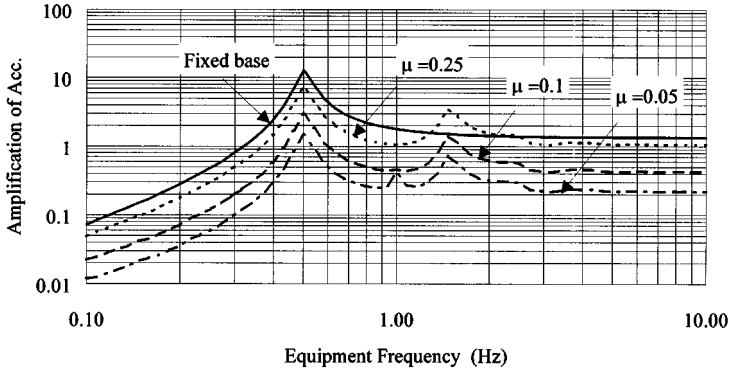

Figure 9. Effect of equipment frequency ($f_g = 0{\cdot}5$ Hz; $f_s = 1$ Hz; $f_s^* = 1{\cdot}15$ Hz)

Earthquake excitation

The dynamic behaviour of an equipment mounted on a sliding structure subjected to harmonic ground motions has been investigated in the preceding subsection. It should be noted that the dynamic characteristics observed for sliding structure under steady-state harmonic excitation may not exist in the presence of earthquake excitation, as the seismic motion of a structural system is of transient nature. This subsection is concentrated on the seismic response of the equipment mounted on a sliding structure.

The first 30-second records of the following three real earthquakes are used in this study: Taft (Taft Lincoln School Tunnel, Kern County, California earthquake, July 1952), El Centro (El Centro site, Imperial Valley earthquake, May 1940), and Pacoima (Pacoima dam, San Fernado earthquake, February 1971) of which the peak ground accelerations (PGA) are listed in Table I. These earthquakes are selected to represent three different seismic intensities, namely, the modest (Taft), the strong (El Centro) and the severe (Pacoima) earthquakes, as can be appreciated from their autospectral density functions[9] and the response spectral curves with 5 per cent damping plotted in Figures 10 and 11, respectively. By imposing the earthquakes with different intensities, the effect of sliding motion on the equipment response can be studied. Again, the focus of the present study will be placed on the three effects, the effect of friction coefficients, subharmonic resonance and the effect of tuning.

Variation of friction coefficients. To illustrate the effect of the frictional coefficient μ, Figure 12 shows the sliding response spectrum of the equipment mounted on the SDOF sliding structural system for different values of μ and subjected to the El Centro earthquake. The results for four different μ values, i.e. $\mu = 0{\cdot}05, 0{\cdot}1,$

Table I. Peak ground accelerations (PGA) of the example earthquakes

Earthquake	Taft	El Centro	Pacoima
PGA (g)	0·18	0·35	1·17

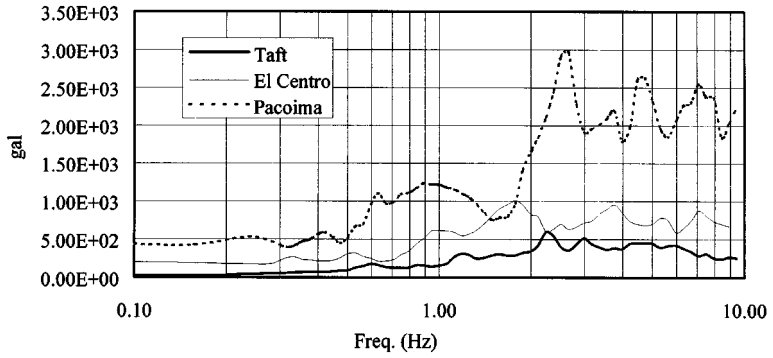

Figure 10. Response spectra of Taft, El Centro and Pacoima (5 per cent damping)

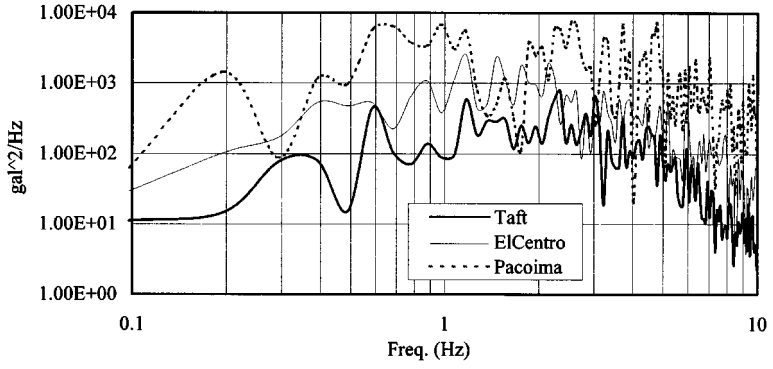

Figure 11. Autospectra of Taft, El Centro and Pacoima (first 30 sec)

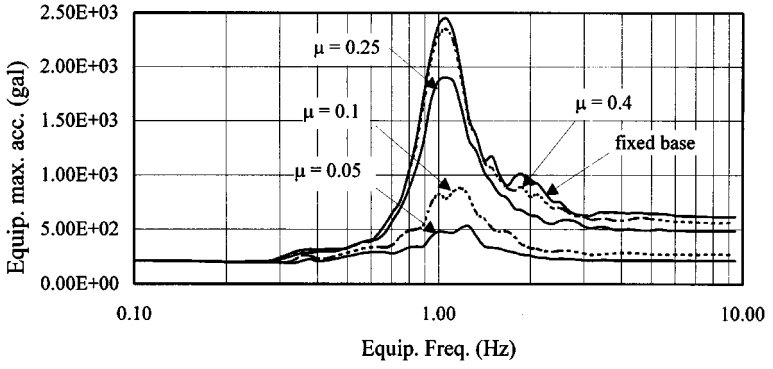

Figure 12. Equipment response excited by El Centro earthquake

0·25 and 0·4, and for the fixed base case ($\mu = \infty$) are shown in Figure 12, in which the equipment frequency considered ranges from 0·1 to 10 Hz. Similar spectral curves are also depicted in Figures 13 and 14 for the Taft and Pacoima earthquakes, respectively.

From the above three figures, one observes that the smaller the μ value, the more the maximum equipment response is reduced. This observation is true for any given equipment frequency. For all of the three earthquakes considered, the equipment response of the fixed base case grows dramatically around the natural frequency of the primary structure (i.e. 1 Hz). Such an effect of magnification can be effectively reduced through the introduction of a sliding support with a relatively small value of μ. However, for a given value of μ, the amount of response reduction varies from one earthquake to another. For instance, installing a sliding support of $\mu = 0{\cdot}25$ does not cause much reduction on the equipment response when subjected to the Taft earthquake (Figure 13), while it can achieve a reduction of as great as 70 per ccent even with a very large μ value, say $\mu = 0{\cdot}4$, when subjected to the Pacoima earthquake (Figure 14). Furthermore, for smaller values of μ, say $\mu = 0{\cdot}05$, the equipment response associated with Pacoima appears to be almost constant. Such a phenomenon implies that the maximum response of the equipment is insensitive to its natural frequency.

Another conclusion from Figures 12–14 is that the sliding support is more effective for mitigating the equipment response in a severe earthquake than in a moderate one. The reason behind this is that for moderate earthquakes the inertia force induced on the super structure may not exceed the maximum static frictional force throughout most of the duration of excitation, which implies that the structure remains in the non-sliding phase for most of the time. Consequently, the equipment response in the sliding structure is very close to that in a fixed base structure.

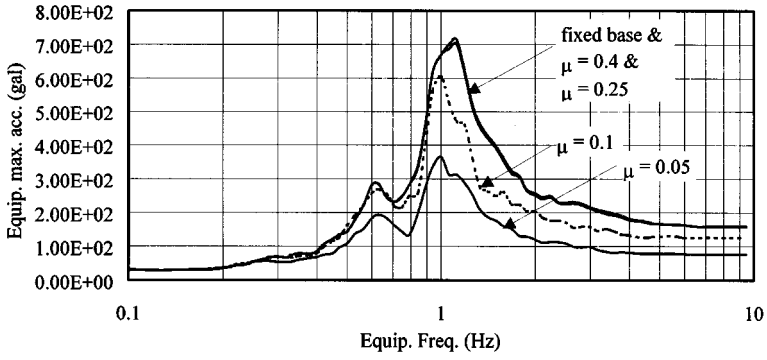

Figure 13. Equipment response excited by Taft earthquake

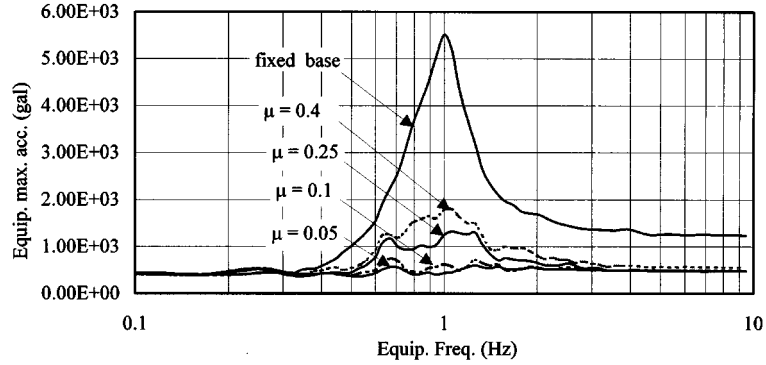

Figure 14. Equipment response excited by Pacoima earthquake

A similar observation can be found in time domain, also. In Figure 15, the time history response of the equipment excited by the El Centro earthquake are plotted for $\mu = 0{\cdot}1$, $0{\cdot}05$ and the fixed base. From the figure, one observes that for the first 15 sec, where the main shock of the earthquake occurs, the sliding support shows its effectiveness in reducing the acceleration levels. However, it becomes rather ineffective afterward, as the ground acceleration is lower than a threshold value, and so the three response curves become almost coincident.

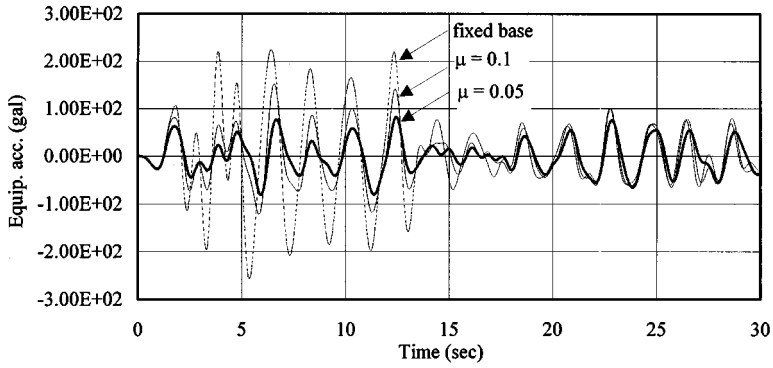

Figure 15. Time history response of equipment for different μ values excited by El Centro earthquake ($f_e = 0{\cdot}5$ Hz)

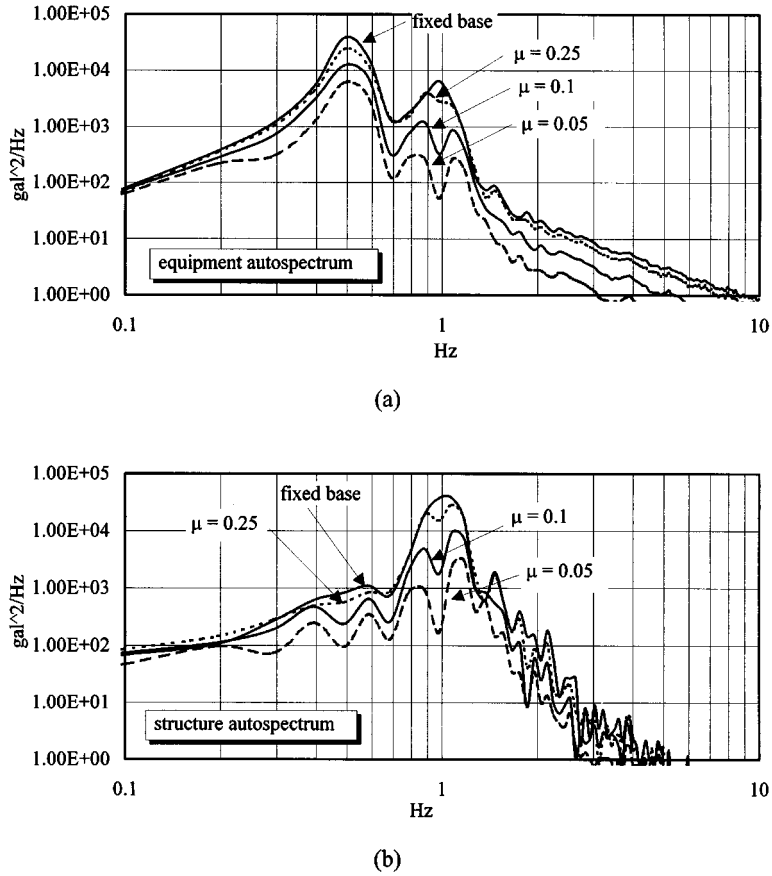

Figure 16. Autospectra of equipment and primary structure excited by El Centro earthquake ($f_e = 0{\cdot}5$ Hz; $f_s = 1$ Hz; $f_s^* = 1{\cdot}15$ Hz)

Subharmonic resonance. As was illustrated in the case of harmonic excitations, the equipment response will exhibit certain subharmonic resonance at frequencies lower than the equipment's natural frequency and, due to this effect, the sliding structure with a relatively high μ value will have a larger equipment response than that of the fixed base case. This subsection aims to investigate whether the same phenomenon can be found in the seismic motion of the equipment.

Now, since an earthquake excites a structure through a wide range of frequency, the seismic response of the structure will be excited across the same range of frequency. In order to see the frequency distribution of the structure response, one may evaluate the spectral density function from the time history response. In this study, the method of autospectrum[9] (autospectral density function) is employed to analyse the seismic response of the mounted equipment in frequency domain. In all cases that follow, only the first 30 sec response of the equipment or the primary structure is taken in the computation for autospectrum curves.

As a beginning, let us compute the autospectrum of the equipment subjected to the El Centro Earthquake. Two equipment frequencies, i.e. $f_e = 0{\cdot}5$ and 5 Hz, are considered to simulate the condition of soft and stiff equipment, respectively.

For the case of $f_e = 0{\cdot}5$ Hz (soft equipment), Figures 16(a) and 16(b) show the autospectrum of the equipment as well as of the primary structure. In both figures, the spectral curves have been plotted for the four sliding support conditions, i.e. $\mu = 0{\cdot}05$, 0·1, 0·25, and the fixed base case. The followings are the observations made from these two figures: (1) for frequencies lower than primary structure's natural frequency (i.e. 1 Hz), the autospectra of the primary structure (Figure 16(a)) with $\mu = 0{\cdot}05$ and 0·1 exhibit several peaks (subharmonic resonance), which, however, are absent from the fixed base case. (2) A comparison of Figures 16(a) with 16(b) shows that the autospectra of the equipment are very different from those of

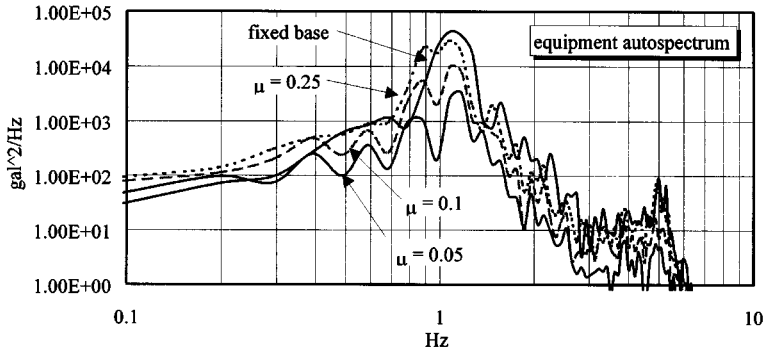

(a)

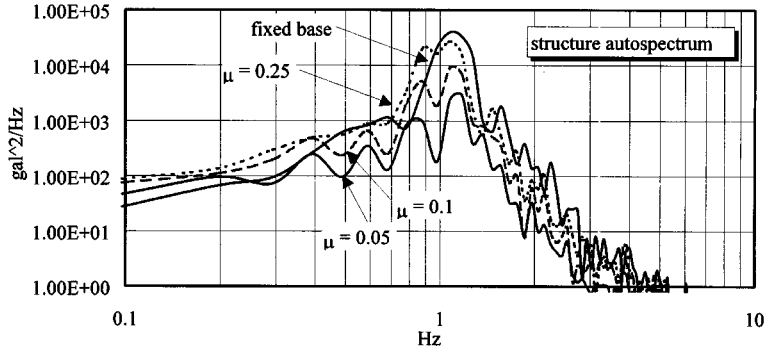

(b)

Figure 17. Autospectra of equipment and primary structure excited by El Centro earthquake ($f_e = 5$ Hz; $f_s = 1$ Hz; $f_s^* = 1{\cdot}15$ Hz)

the structure. The subharmonic phenomenon observed in the structure's autospectra does not appear in the equipment's, implying that it does not have much effect on the equipment's response. (3) The frequency content of the equipment response is mainly concentrated at around the equipment's natural frequency and the structure's resonance frequency. However, slight variations occur around the latter depending on the μ value selected, which are similar to those observed in the study of harmonic excitation.

As for the stiff equipment case ($f_e = 5$ Hz), the autospectra of the equipment and the structure have been plotted in Figures 17(a) and 17(b), respectively. Comparison of these two figures shows that the autospectra of the equipment are almost identical to those of the structure for the various μ values selected, except that the former show a higher response around the equipment frequency (5 Hz). Such a fact implies that for a relative stiff equipment, the dynamic effect contributed by the equipment itself is insignificant. Moreover, for the present case, the subharmonic resonance has equal influence on the structure and equipment responses.

Both the Taft and Pacoima earthquakes are also considered in the study of the soft equipment case (i.e. with $f_e = 0{\cdot}5$ Hz). Based on the autospectra of the equipment depicted in Figures 18 and 19, the following observations can be made: (1) For a moderate earthquake, such as Taft, the autospectra of both the equipment and the structure do not vary significantly from those of the fixed base case for all the μ values considered. Therefore, no subharmonic effect are observed. (2) For a severe earthquake, such as Pacoima, the autospectra of both the equipment and the structure show considerable difference for different values of μ. The subharmonic resonance can be observed for the structure for the frequencies lower than 1 Hz, but not for the equipment. (3) Figure 19(a) shows a trend very similar to that of Figure 4 for harmonic excitation. All the

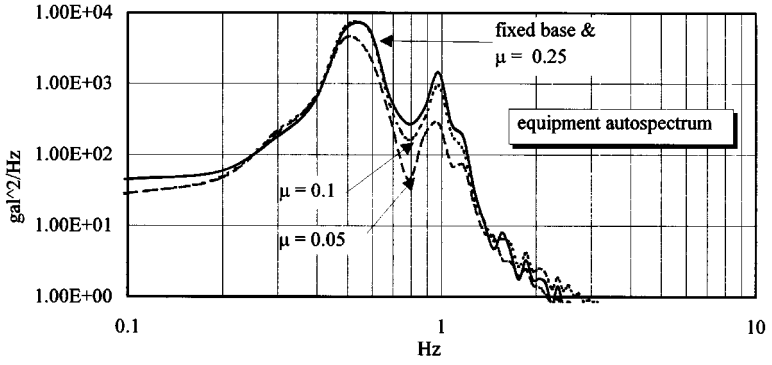

(a)

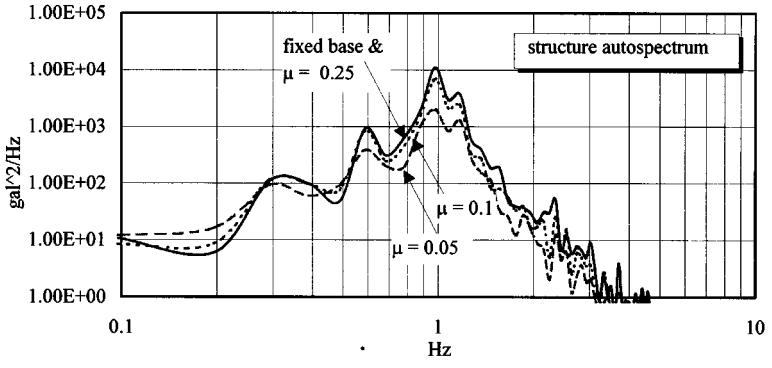

(b)

Figure 18. Autospectra of equipment and primary structure excited by Taft earthquake ($f_e = 0{\cdot}5$ Hz; $f_s = 1$ Hz; $f_s^* = 1{\cdot}15$ Hz)

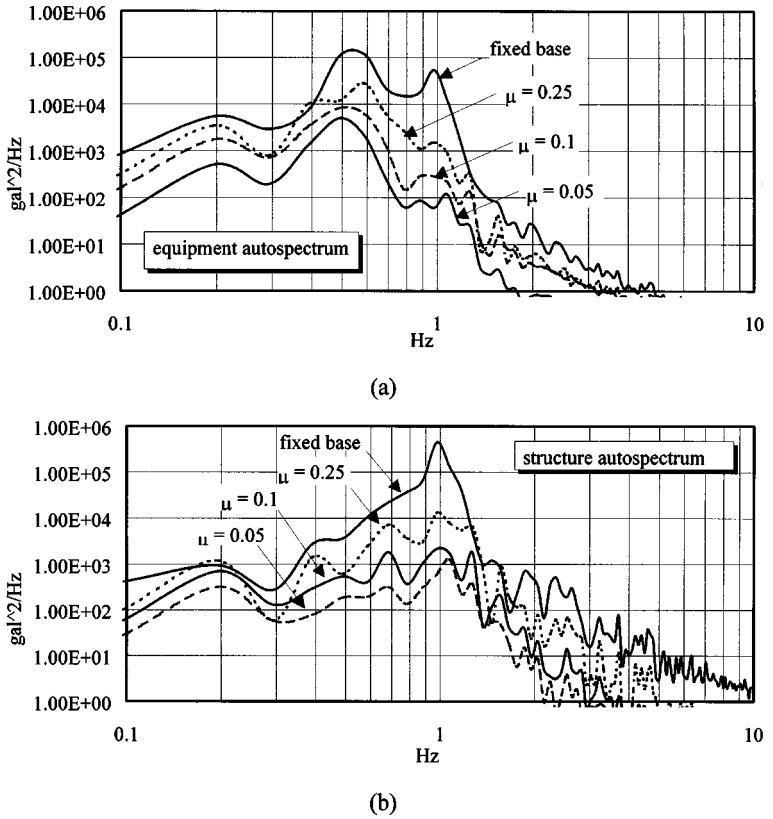

Figure 19. Autospectra of equipment and primary structure excited by Pacoima earthquake ($f_e = 0{\cdot}5$ Hz; $f_s = 1$ Hz; $f_s^* = 1{\cdot}15$ Hz)

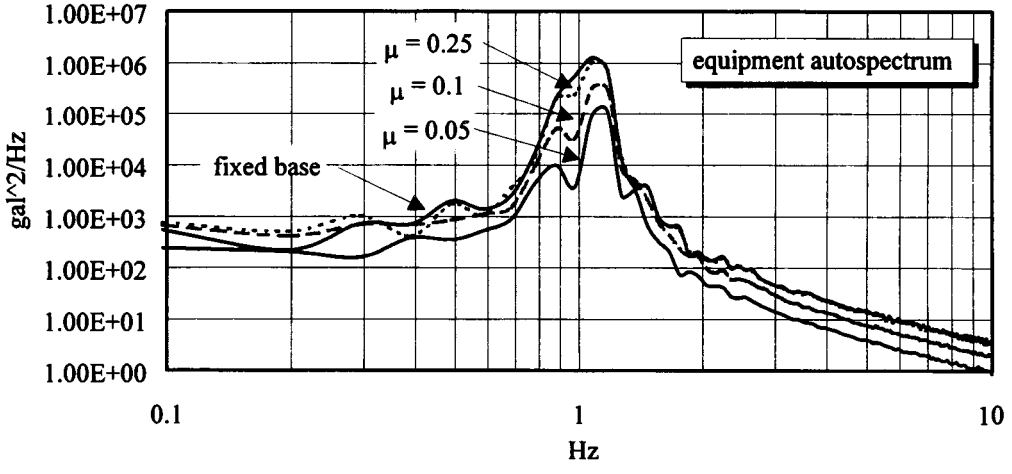

Figure 20. Tuned equipment autospectra excited by El Centro earthquake ($f_e = 1{\cdot}1$ Hz; $f_s = 1$ Hz; $f_s^* = 1{\cdot}15$ Hz)

curves in both figures have larger responses around the equipment frequency (0·5 Hz) and structural frequency (1 Hz), and the implementation of sliding supports is more effective in reducing the part of the response associated with the structural frequency, rather than with the equipment frequency.

Effect of tuning. The tuning effect occurs when the frequency of the equipment is tuned to that of the primary structure. The response spectra shown in Figures 12–14 for the three earthquakes may help us

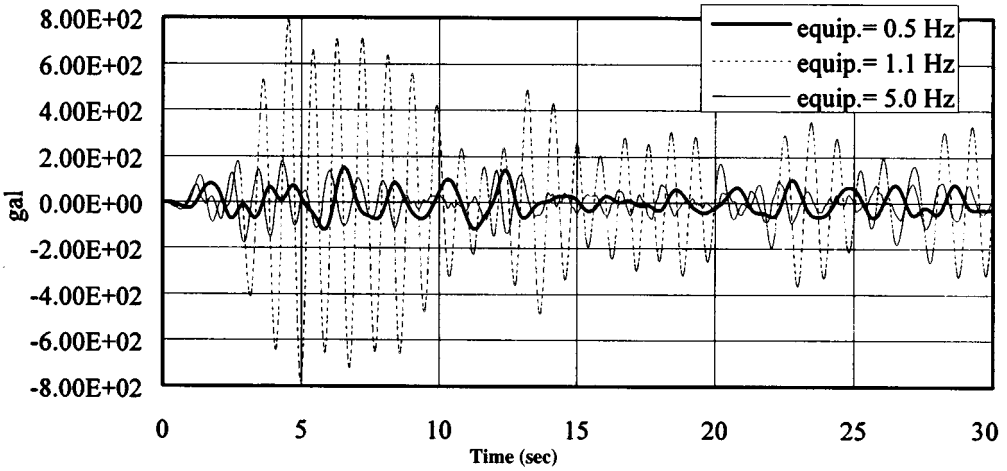

Figure 21. Time history response of equipment excited by El Centro earthquake for different equipment frequencies ($\mu = 0{\cdot}1$)

explain how the tuning affects the equipment response. From these three figures, it can be seen that for the fixed base case the maximum equipment response is dramatically magnified at the frequency where tuning occurs, and that by using a relatively small value of μ, this magnification can be mitigated and even removed. In particular, one notes from Figure 14 that the sliding support is very effective means for protecting the equipment against severe earthquakes, such as Pacoima, regardless of the occurrence of tuning.

Consider the tuning case in which $f_e = 1{\cdot}1$ Hz (note that $f_s = 1$ Hz and $f_s^* = 1{\cdot}15$ Hz), The autospectra shown in Figure 20 for the equipment excited by the El Centro earthquake for the tuned case is to be compared with the untuned cases shown in Figures 16(a) and 17(a). To make it clear, the time histories for all the tuned and untuned cases have been plotted in Figure 21 for $\mu = 0{\cdot}1$. From these, one observes that: (1) The response of the equipment is considerably magnified around the tuned frequency, 1·1 Hz, even with a relatively small μ, say 0·1. (2) For the tuned equipment, no significant magnification occurs with the response in the lower frequency range, where subharmonic resonance has been observed in the study of harmonic excitation.

CONCLUSIONS

The dynamic behaviour of a single DOF equipment mounted on a sliding primary structure subjected to both harmonic and earthquake ground motions has been studied. A systematic numerical procedure capable of simulating a multi-DOF sliding structural system, which is of non-linear nature, is proposed. Two numerical examples have been prepared mainly to investigate the three effects on the equipment response, namely, subharmonic resonance, variation of frictional coefficients and tuning effect. From these examples, the following observations can be made. (1) In general, the introduction of a sliding foundation into a structural system is effective in reducing the response of the mounted equipment as compared with the equipment response in a fixed base structure. In most cases, the reduction level increases when a smaller frictional coefficient of the sliding foundation is applied. Also, the degree of reduction grows as the severity of the earthquake increases. (2) In the study of harmonic excitation, the phenomenon of subharmonic resonance, which occurs exclusively when the excitation frequencies are lower than the equipment frequency, is clearly observed. Due to the presence of this phenomenon, the equipment responses at the subharmonic resonant frequencies are higher than those of the fixed base case, if a larger frictional coefficient is adopted. On the other hand, no significant subharmonic resonance can be observed for the case of earthquake excitation. (3) For both harmonic and earthquake excitations, the frequency domain analysis indicates that the sliding support is more effective in reducing the equipment motion associated with the resonant

frequency of the primary structure, rather than that associated with the natural frequency of the equipment itself. Moreover, the resonant frequency of the primary structure varies with the selection of frictional coefficients. (4) For an equipment tuned to the main resonant frequency of the primary structure, its response can be dramatically magnified. For the case of harmonic excitation, the equipment response is magnified at both main and subharmonic resonant frequencies. The magnification can be mitigated or even removed using a sliding support with a small coefficient of friction.

ACKNOWLEDGEMENTS

This research is sponsored in part by the National Science Council of the Republic of China under Grant No. NSC 82-0410-E002-101.

REFERENCES

1. B. Westermo and F. Udwadia, 'Period response of a sliding oscillator system to harmonic excitation', *Earthquake eng. struct. dyn.* **11**, 135–146 (1983).
2. N. Mostaghel, M. Hejazi and J. Tanbakuchi, 'Response of sliding structures to harmonic support motion', *Earthquake eng. struct. dyn.* **11**, 355–366 (1983).
3. N. Mostaghel and J. Tanbakuchi, 'Response of sliding structures to earthquake support motion', *Earthquake eng. struct. dyn.* **11**, 729–748 (1983).
4. M. Qamaruddin, Rasheeduzzafar, A. S. Arya and B. Chandra, 'Seismic response of masonry buildings with sliding substructure', *J. struct. eng. ASCE* **112**, 2001–2011 (1986).
5. A. G. Hernried and K. M. Lei, 'Parametric studies on the response of equipment in resilient-friction base isolated structures subjected to ground motion', *Int. j. eng.* **struct.** *Vol.* **15**, No. 5, 349–357 (1993).
6. Y. B.Yang, T. Y. Lee and I. C. Tsai , 'Response of multi-degree-of-freedom structures with sliding supports', *Earthquake eng. struct. dyn.* **19**, 739–752 (1990).
7. L. Y. Lu and Y. B. Yang, 'Dynamic characteristics of equipment in sliding structures', *Proc. 7th Canadian Conf. on earthquake engineering*, Montreal, Quebec, 5–7 June 1995, pp. 237–244.
8. L. Meirovitch, *Computational Methods in Structural Dynamics*, Sijthoff & Noordhoff, Netherlands, 1980.
9. J. Bendat and A. Piersol, *Engineering Applications of Correlation and Spectral Analysis*, 2nd ed., Wiley, New York, 1993.